The Accuracy and Efficiency of Semi-Implicit Time Stepping for Mesoscale Storm Dynamics

S. J. THOMAS

Scientific Computing Division, National Center for Atmospheric Research, Boulder, Colorado

G. L. BROWNING

NOAA/Forecast Systems Laboratory, Boulder, Colorado

(Manuscript received 28 July 2000, in final form 13 March 2001)

ABSTRACT

The semi-implicit time-stepping scheme is often applied to the terms responsible for fast waves in large-scale global weather prediction and general circulation models to remove the time step restrictions associated with these waves. Both the phase and amplitude of fast gravity waves are distorted in such models. Because gravity waves carry very little energy, this distortion does not significantly impact the large-scale flow. At mesoscale resolutions the semi-implicit scheme can also be applied, but it has been generally assumed that the treatment of gravity waves is inaccurate at these scales as well. In this paper mesoscale convective systems in the midlatitudes driven by diabatic heating are studied. According to a recently developed mathematical theory, only gravity waves with wavelengths larger than the characteristic length scale of the heat source contain a significant amount of energy, and here it is shown that these gravity waves are accurately reproduced by a semi-implicit discretization of the 3D compressible governing equations with a time step appropriate for the dominant solution component. It will also be shown that the structure equation reduces to the gravity wave equation of the mathematical theory when the appropriate scaling arguments are applied.

1. Introduction

The semi-implicit time-stepping scheme is often applied to the terms responsible for fast waves in large-scale global weather prediction and general circulation models to remove the time step restrictions associated with these waves (e.g., Williamson and Laprise 1999). Both the phase and amplitude of the fastest gravity waves are severely distorted in such numerical models. Because these waves carry very little energy, this distortion does not significantly impact the large-scale flow. An early paper analyzing the semi-implicit method in the context of a heat conduction problem is Johansson and Kreiss (1963). In meteorology, the semi-implicit method was first introduced by Robert (1969) and Kwizak and Robert (1971). Elvius and Sundström (1973) analyzed the stability and accuracy of the scheme for the shallow water equations in periodic and limited-area domains and proposed well-posed boundary conditions for the latter. The semi-implicit scheme has also been applied at mesoscale resolutions (Tapp and White 1976; Cullen 1990; Tanguay et al. 1990; Golding 1992) and at convective scales by Robert (1993). However, it is generally assumed that the treatment of gravity waves is inaccurate at these scales as well and an error analysis for the nonhydrostatic compressible equations analogous to Elvius and Sundström (1973) has not appeared to date in the literature.

Recently Browning and Kreiss (1997) have developed a mathematical theory proposing that a midlatitude mesoscale storm driven by cooling and heating consists of two components that do not interact significantly with each other. The dominant component of the solution contains most of the energy in the vicinity of the storm and is meteorologically significant. The second solution component consists of large-scale gravity waves that have the same time and depth scales and the same amplitude of pressure perturbations as the dominant component. These gravity waves propagate horizontally away from the storm and can last for a considerable period of time after the storm has dissipated. This theory does not rely on the normal modes of the homogeneous system, but rather is based on a scaling of the equations in physical space, that is, on the standard bounded derivative theory approach (Kreiss 1979, 1980). Thus, the new theory is applicable in the troposphere both inside and outside the region of diabatic heating.

An important question is whether or not large-scale gravity waves generated by a mesoscale storm can be

Corresponding author address: Dr. S. J. Thomas, Scientific Computing Division, NCAR, 1850 Table Mesa Drive, Boulder, CO 80307. E-mail: thomas@ucar.edu

© 2001 American Meteorological Society

resolved by a particular numerical model. The purpose of this paper is to prove mathematically and demonstrate with computer simulations that a 3D semi-implicit time discretization scheme for the nonhydrostatic compressible governing equations can accurately reproduce both the dominant and gravity wave components of the solution at a computational cost, which is competitive with the multiscale system of Browning and Kreiss (1986, 1994). Indeed, it seems reasonable to expect that a time step chosen for sufficient accuracy of the dominant component might also produce accurate approximations of the large-scale gravity waves because these waves have the same timescale as the dominant component. Essentially it will be shown that the semi-implicit scheme can accurately reproduce gravity waves with wavelengths larger than the characteristic length scale of the heat source. This result also fits directly into the Browning and Kreiss (1997) theory because the structure equation reduces to the simplified gravity wave equation of their theory when the appropriate scaling arguments are applied. The reduced system of equations described by the authors can be used to simulate the dominant component of the mesoscale solution.

The outline of this paper is as follows. Section 2 contains the scaling of the 3D compressible governing equations associated with midlatitude mesoscale convective systems (MCSs). For comparison purposes, it is shown that the structure equation for the full 3D system reduces to the gravity wave equation when the appropriate scaling arguments are employed. Fourier analysis of the full system provides the continuous eigenvalues that are needed for error estimates. Section 3 presents an analysis of the stability and accuracy of the semi-implicit scheme. Section 4 provides details of the semi-implicit discretization and presents an $O(N^3 \log N)$ fast elliptic solver. Finally, section 5 contains simulation results for a theoretical forcing function that closely matches observed MCS characteristic scales. Here it is shown that the semi-implicit solution closely matches an explicit simulation.

2. Mesoscale dynamics

In this paper we consider the nonhydrostatic fully compressible governing equations as specified in Browning and Kreiss (1986). The model is formulated with respect to a horizontally homogeneous time invariant, and hydrostatically balanced base-state reference atmosphere. Thermodynamic variables are decomposed into a sum of the base state and perturbations:

$$s = s'[s_0(z) + 1], \qquad p = p_0(z) + p',$$
$$\rho = \rho_0(z) + \rho',$$

where

$$\frac{\partial p_0}{\partial z} = -g\rho_0 = -\frac{gp_0}{RT_0},$$

and the equation of state is $p_0(z) = \rho_0(z)RT_0(z)$. The gas constant for dry air is R, $\gamma = c_p/c_v$, and $c_p - c_v = R$.

After introduction of the base-state, the prognostic equations for momentum (u, v, w), perturbation pressure p', and thermodynamic perturbation s' are given by

$$\frac{du}{dt} + \frac{1}{\rho_0}\frac{\partial p'}{\partial x} - fv = 0$$
$$\frac{dv}{dt} + \frac{1}{\rho_0}\frac{\partial p'}{\partial y} - fu = 0$$
$$\frac{dw}{dt} + \frac{1}{\rho_0}\frac{\partial p'}{\partial z} - B = 0$$
$$\frac{ds'}{dt} - \tilde{s}(w - H) = 0$$
$$\frac{dp'}{dt} + p_0\gamma D - g\rho_0 w = G,$$

where B is the buoyancy, D is the divergence, f is the Coriolis parameter, and H and G represent heat sources. The Exner function is $\pi = (p/p_{00})^{R/c_p}$ and $s = \rho p^{-1/\gamma}$ is inversely proportional to the potential temperature $\theta = T/\pi$,

$$\theta = T\left(\frac{p_{00}}{p}\right)^{1-1/\gamma}, \qquad \theta^{-1} = \frac{R}{p_{00}^{R/c_p}}\rho p^{-1/\gamma} = \alpha s.$$

The Brunt–Väisällä frequency N_0^2 and stratification parameter $\tilde{s}$ are defined as follows:

$$N_0^2 = g\tilde{s}, \qquad \tilde{s} = -\frac{1}{s_0}\frac{\partial s_0}{\partial z} = \frac{1}{\theta_0}\frac{\partial \theta_0}{\partial z}.$$

The buoyancy B in the vertical motion equation is derived by expanding the inverse of potential temperature in a Taylor series about the reference state

$$(\theta_0 + \theta')^{-1} = \alpha(\rho_0 + \rho')(p_0 + p')^{-1/\gamma}$$

and retaining the first-order terms

$$\theta_0^{-1}\left(1 - \frac{\theta'}{\theta_0}\right) = \alpha\rho_0 p_0^{-1/\gamma}\left(1 + \frac{\rho'}{\rho_0} - \frac{1}{\gamma}\frac{p'}{p_0}\right).$$

Simplifying, it follows that

$$-\frac{\theta}{\theta_0} = s' = \frac{\rho'}{\rho_0} - \frac{1}{\gamma}\frac{p'}{p_0}$$

and therefore the buoyancy is given by

$$B(s', p') = -(gs' + \tilde{p}p'), \qquad \tilde{p} = \frac{g}{\gamma p_0}.$$

For the characteristic scales of the mesoscale motions analyzed by Browning and Kreiss (1986, 1994, 1997), the corresponding set of scaled governing equations is

$$\frac{du}{dt} + \frac{1}{\rho_0}\frac{\partial p'}{\partial x} - fv = 0$$

$$\frac{dv}{dt} + \frac{1}{\rho_0}\frac{\partial p'}{\partial y} + fu = 0$$

$$\frac{dw}{dt} + \varepsilon^{-2}\frac{1}{\rho_0}\frac{\partial p'}{\partial z} - \varepsilon^{-2}B = 0$$

$$\frac{ds'}{dt} - \varepsilon^{-2}\tilde{s}(w - H) = 0$$

$$\frac{dp'}{dt} + \varepsilon^{-3}p_0\gamma D - \varepsilon^{-3}g\rho_0 w = \varepsilon^{-2}G.$$

The same notation is used for both dimensional and nondimensional variables. Parameters like the Rossby number are replaced by the appropriate power of $\varepsilon = 0.1$. The reduced system of Browning and Kreiss (1986, 1994, 1997) is derived by using the balance between the vertical velocity and heating that must occur for slowly evolving mesoscale solutions. Replacing w by H in the time-dependent equations for u, v, and p and then neglecting small terms (which is permissible because it can be proved that for slowly evolving solutions, space and time derivatives that are initially of order unity will remain so for the timescale of the motion), the reduced system is

$$\frac{du}{dt} + \frac{1}{\rho_0}\frac{\partial p'}{\partial x} - fv = 0$$

$$\frac{dv}{dt} + \frac{1}{\rho_0}\frac{\partial p'}{\partial y} + fu = 0$$

$$\frac{\partial u}{\partial t} + \frac{\partial v}{\partial y} = RF_p,$$

where $d/dt = \partial/\partial t + u\partial/\partial x + v\partial/\partial y + H\partial/\partial z$ and $F_p = -H_z + \tilde{p}\rho_0 H$. Here R is a projection operator that removes the long horizontal waves of F_p when the lateral dimensions of the domain are much larger than the heating. These waves are instead resolved in the gravity wave equation derived below.

We now derive the structure equation for the unforced system, as has been standard practice, then examine the impact of adding a mesoscale heating term. Consider the linearized equations with Coriolis terms neglected (they can be treated explicitly because they are a small part of the fast modes):

$$\frac{\partial u}{\partial t} + \frac{1}{\rho_0}\frac{\partial p'}{\partial x} = 0 \tag{2.1}$$

$$\frac{\partial v}{\partial t} + \frac{1}{\rho_0}\frac{\partial p'}{\partial y} = 0 \tag{2.2}$$

$$\frac{\partial w}{\partial t} + \varepsilon^{-2}\frac{1}{\rho_0}\frac{\partial p'}{\partial z} - \varepsilon^{-2}B = 0 \tag{2.3}$$

$$\frac{\partial s'}{\partial t} - \varepsilon^{-2}\tilde{s}w = 0 \tag{2.4}$$

$$\frac{\partial p'}{\partial t} + \varepsilon^{-3}p_0\gamma D - \varepsilon^{-3}g\rho_0 w = 0. \tag{2.5}$$

The derivation is easily carried out in Fourier space for periodic domains. However, it is presented here in physical space for comparison with the new theory and numerical algorithms. First, the buoyancy B is eliminated from the equations, resulting in

$$\left(\varepsilon^{-2}N_0^2 + \varepsilon^2\frac{\partial^2}{\partial t^2}\right)w + \frac{1}{\rho_0}\left(\frac{\partial}{\partial z} + \frac{g}{c_0^2}\right)\frac{\partial p'}{\partial t} = 0. \tag{2.6}$$

The next step in the derivation of the structure equation is to eliminate the divergence D from the system of equations, which leads to the equation

$$\frac{1}{\rho_0}\left(\frac{\varepsilon^3}{c_0^2}\frac{\partial^2}{\partial t^2} - \nabla_h^2\right)p' + \left(\frac{\partial}{\partial z} - \frac{g}{c_0^2}\right)\frac{\partial w}{\partial t} = 0. \tag{2.7}$$

To eliminate w from the equations,

$$\left(\varepsilon^{-2}N_0^2 + \varepsilon^2\frac{\partial^2}{\partial t^2}\right)(2.7) - \left(\frac{\partial}{\partial z} - \frac{g}{c_0^2}\right)\frac{\partial}{\partial t}(2.6)$$

and an equation for p' is obtained

$$\left(\varepsilon^{-2}N_0^2 + \varepsilon^2\frac{\partial^2}{\partial t^2}\right)\frac{1}{\rho_0}\left(\frac{\varepsilon^3}{c_0^2}\frac{\partial^2}{\partial t^2} - \nabla_h^2\right)p' - \left(\frac{\partial}{\partial z} - \frac{g}{c_0^2}\right)\frac{1}{\rho_0}\left(\frac{\partial}{\partial z} - \frac{g}{c_0^2}\right)\frac{\partial^2 p'}{\partial t^2} = 0. \tag{2.8}$$

For isothermal T_0, divide (2.8) by RT_0 and apply the relation

$$\left(\frac{\partial}{\partial z} - \frac{g}{c_0^2}\right)\frac{1}{p_0} = \frac{1}{p_0}\left(\frac{\partial}{\partial z} + \frac{g}{RT_0} - \frac{g}{c_0^2}\right) = \frac{1}{p_0}\left(\frac{\partial}{\partial z} + \frac{N_0^2}{g}\right)$$

to obtain the scaled equation

$$\left(\varepsilon^{-2}N_0^2 + \varepsilon^2\frac{\partial^2}{\partial t^2}\right)\left(\frac{\varepsilon^3}{c_0^2}\frac{\partial^2}{\partial t^2} - \nabla_h^2\right)p' - \left(\frac{\partial}{\partial z} - \frac{N_0^2}{g}\right)\left(\frac{\partial}{\partial z} + \frac{g}{c_0^2}\right)\frac{\partial^2 p'}{\partial t^2} = 0. \tag{2.9}$$

Following Browning et al. (2000), assume that $\partial w/\partial t = 0$ in (2.3), $g\rho_0 w = 0$ in (2.5), and define $\phi' = p'/\rho_0$. Then the scaled equation becomes

$$\varepsilon\frac{N_0^2}{c_0^2}\frac{\partial^2}{\partial t^2}\phi' - \varepsilon^{-2}N_0^2\nabla_h^2\phi' - \frac{\partial^2}{\partial z^2}\frac{\partial^2}{\partial t^2}\phi' = 0. \tag{2.10}$$

This equation is identical to the gravity wave equation (3.4) in Browning et al. (2000) when the heat source H is included

$$\left[-c_0^2(g\tilde{s})^{-1}\frac{\partial^2}{\partial z^2} + \varepsilon\right]\frac{\partial^2\phi'}{\partial t^2} - \varepsilon^{-2}c_0^2\nabla_h^2\phi' = -\varepsilon^{-2}c_0^2\frac{\partial}{\partial z}\frac{\partial}{\partial t}H. \tag{2.11}$$

In order to obtain error estimates in the following section, symmetrize the governing equations using the transformation

$$f_1\bar{u} = u, \qquad f_2\bar{v} = v, \qquad f_3\bar{w} = w, \qquad f_4\bar{s} = s',$$
$$f_5\bar{p} = p',$$

where

$$f_1 = \varepsilon^{3/2}e^{\Gamma z}, \qquad f_2 = \varepsilon^{3/2}e^{\Gamma z}, \qquad f_3 = \varepsilon^{1/2}e^{\Gamma z},$$
$$f_4 = \frac{N_0}{g}f_3, \qquad f_5 = c_0\rho_0 e^{\Gamma z}, \quad \text{and}$$
$$(\gamma p_0\rho_0)^{1/2} = c_0\rho_0, \qquad \Gamma = \frac{g}{2RT_0}, \qquad S = c_0\left(-\Gamma + \frac{g}{c_0^2}\right).$$

The above diagonal similarity transformation leads to the symmetric hyperbolic system

$$\frac{d\bar{u}}{dt} + \varepsilon^{-3/2}c_0\frac{\partial\bar{p}}{\partial x} = 0$$
$$\frac{d\bar{v}}{dt} + \varepsilon^{-3/2}c_0\frac{\partial\bar{p}}{\partial y} = 0$$
$$\frac{d\bar{w}}{dt} + \varepsilon^{-5/2}c_0\frac{\partial\bar{p}}{\partial z} + \varepsilon^{-5/2}S\bar{p} + \varepsilon^{-2}N_0\bar{s} = 0$$
$$\frac{d\bar{s}}{dt} - \varepsilon^{-2}N_0\bar{w} = 0$$
$$\frac{d\bar{p}}{dt} + \varepsilon^{-3/2}c_0\frac{\partial\bar{u}}{\partial x} + \varepsilon^{-5/2}c_0\frac{\partial\bar{w}}{\partial z} - \varepsilon^{-5/2}S\bar{w} = 0,$$

which can be written as

$$\frac{\partial\mathbf{u}}{\partial t} + A_1\frac{\partial\mathbf{u}}{\partial x} + A_2\frac{\partial\mathbf{u}}{\partial y} + A_3\frac{\partial\mathbf{u}}{\partial z} + B\mathbf{u} = 0,$$

where $\mathbf{u} = (\bar{u}, \bar{v}, \bar{w}, \bar{s}, \bar{p})$ and

$$\mathbf{A}_1 = \begin{bmatrix} u_0 & 0 & 0 & 0 & \varepsilon^{-3/2}c_0 \\ 0 & u_0 & 0 & 0 & 0 \\ 0 & 0 & u_0 & 0 & 0 \\ 0 & 0 & 0 & u_0 & 0 \\ \varepsilon^{-3/2}c_0 & 0 & 0 & 0 & u_0 \end{bmatrix},$$

$$\mathbf{A}_2 = \begin{bmatrix} v_0 & 0 & 0 & 0 & 0 \\ 0 & v_0 & 0 & 0 & \varepsilon^{-3/2}c_0 \\ 0 & 0 & v_0 & 0 & 0 \\ 0 & 0 & 0 & v_0 & 0 \\ 0 & \varepsilon^{-3/2}c_0 & 0 & 0 & v_0 \end{bmatrix},$$

$$\mathbf{A}_3 = \begin{bmatrix} w_0 & 0 & 0 & 0 & 0 \\ 0 & w_0 & 0 & 0 & 0 \\ 0 & 0 & w_0 & 0 & \varepsilon^{-5/2}c_0 \\ 0 & 0 & 0 & w_0 & 0 \\ 0 & 0 & \varepsilon^{-5/2}c_0 & 0 & w_0 \end{bmatrix},$$

$$\mathbf{B} = \begin{bmatrix} 0 & 0 & 0 & 0 & 0 \\ 0 & 0 & 0 & 0 & 0 \\ 0 & 0 & 0 & \varepsilon^{-2}N_0 & \varepsilon^{-5/2}S \\ 0 & 0 & -\varepsilon^{-2}N_0 & 0 & 0 \\ 0 & 0 & -\varepsilon^{-5/2}S & 0 & 0 \end{bmatrix}.$$

Applying the Fourier transformation in space, with $\mathbf{k} = (k, l, m)$ being the real dual variable and a hat denoting the transform of a variable, the system becomes

$$\frac{\partial\hat{\mathbf{u}}}{\partial t} + i\mathbf{A}(\mathbf{k})\hat{\mathbf{u}} + idI\hat{\mathbf{u}} = 0, \tag{2.12}$$

where $d = u_0k + v_0l + w_0m$,

$$\mathbf{A}(\mathbf{k}) = \begin{bmatrix} 0 & 0 & 0 & 0 & \varepsilon^{-3/2}c_0k \\ 0 & 0 & 0 & 0 & \varepsilon^{-3/2}c_0l \\ 0 & 0 & 0 & i\varepsilon^{-2}N_0 & \varepsilon^{-5/2}(c_0m + iS) \\ 0 & 0 & i\varepsilon^{-2}N_0 & 0 & 0 \\ \varepsilon^{-3/2}c_0k & \varepsilon^{-3/2}c_0l & \varepsilon^{-5/2}(c_0m + iS) & 0 & 0 \end{bmatrix}$$

and $i\mathbf{A}(\mathbf{k}) + idI$ is the symbol of the spatial part of the PDE. Given that the coefficient matrices $\mathbf{A}_i$ are symmetric, and $\mathbf{B}$ is skew-symmetric, it is possible to find a unitary similarity transformation $\mathbf{P}$ that diagonalizes the Hermitian matrix $\mathbf{A}$, that is, $\mathbf{PAP}^{-1} = \mathbf{\Lambda}$, where $\mathbf{P}^{-1} = \overline{\mathbf{P}}^T = \mathbf{P}^*$ and $\mathbf{\Lambda}$ is a diagonal matrix. Multiplying (2.13) by $\mathbf{P}$,

$$\frac{\partial\mathbf{P}\hat{\mathbf{u}}}{\partial t} + i\mathbf{\Lambda}(\mathbf{k})\mathbf{P}\hat{\mathbf{u}} + idI\mathbf{P}\hat{\mathbf{u}} = 0.$$

Each component of $\mathbf{P}\hat{\mathbf{u}}$ is decoupled from the other components and the jth component of $\mathbf{P}\hat{\mathbf{u}}$ in the homogeneous case varies as $\exp(i\lambda_j t)$, where λ_j is the jth eigenvalue of $i\mathbf{A} + idI$.

Thus to determine the time behavior of the components of $\mathbf{P}\hat{\mathbf{u}}$, it is necessary to determine the roots of the characteristic polynomial of the symbol of the operator. The eigenvalues of $\mathbf{A}$ are roots of the equation

$$\det(\mathbf{A} - \lambda I) = 0$$

and the eigenvalues of $\mathbf{A} + dI$ are $\lambda' = \lambda + d$. The resulting fifth-degree polynomial has a root $\lambda = 0$, corresponding to advection, and the eigenvalues associated with fast modes are roots of the quartic

$$\frac{\lambda^4}{c_0^2} - \varepsilon^{-5}\lambda^2\left[\varepsilon^2(k^2 + l^2) + m^2 + \frac{S^2 + \varepsilon N_0^2}{c_0^2}\right] + \varepsilon^{-7}N_0^2(k^2 + l^2) = 0.$$

Solving the above quartic for λ^2,

$$\lambda^2 \approx \varepsilon^{-5}\frac{c_0^2}{2}\left[\varepsilon^2(k^2 + l^2) + m^2 + \frac{S^2 + \varepsilon N_0^2}{c_0^2}\right] \pm \varepsilon^{-5}\frac{c_0^2}{2}\left\{\left[\varepsilon^2(k^2 + l^2) + m^2 + \frac{S^2 + \varepsilon N_0^2}{c_0^2}\right]^2 - 4\varepsilon^3\frac{N_0^2(k^2 + l^2)}{c_0^2}\right\}^{1/2}.$$

Because $\varepsilon^3 \ll 1$ the first term inside the square root is much larger than the second term and thus choosing the positive sign above leads to an expression for the eigenvalues associated with acoustic waves

$$\lambda^2 \approx \varepsilon^{-5}c_0^2[\varepsilon^2(k^2 + l^2) + m^2] + \varepsilon^{-5}(S^2 + \varepsilon N_0^2).$$

The negative sign leads to eigenvalues corresponding to gravity waves:

$$\lambda^2 \approx \frac{\varepsilon^{-2}N_0^2(k^2 + l^2)}{\varepsilon^2(k^2 + l^2) + m^2 + (S^2 + \varepsilon N_0^2)/c_0^2} \equiv \varepsilon^{-2}\lambda_g^2.$$

For an analysis of the stability and accuracy of gravity waves we have introduced $\lambda = \varepsilon^{-1}\lambda_g$, where $\lambda_g = O(1)$ for this particular scaling of the equations.

3. Stability and accuracy

The stability and accuracy of the semi-implicit scheme are analyzed in this section. To simplify the analysis, we will assume discretization in space employs centered second-order finite differences on an Arakawa C grid. Finite differences result in approximate wave numbers in Fourier space, for example,

$$\tilde{d} = u_0\tilde{k} + v_0\tilde{l} + w_0\tilde{m}, \qquad \tilde{k} = \frac{\sin(k\Delta x)}{\Delta x},$$

$$\tilde{l} = \frac{\sin(l\Delta y)}{\Delta y}, \qquad \tilde{m} = \frac{\sin(m\Delta z)}{\Delta z}.$$

A three-time-level semi-implicit time discretization of the governing equations is equivalent to a Crank–Nicholson scheme applied to the off-diagonal terms combined with an explicit leapfrog scheme for the diagonal (advection) terms:

$$\frac{\hat{\mathbf{v}}^{n+1} - \hat{\mathbf{v}}^{n-1}}{2\Delta t} + i\tilde{A}\frac{\hat{\mathbf{v}}^{n+1} + \hat{\mathbf{v}}^{n-1}}{2} + i\tilde{d}I\hat{\mathbf{v}}^n = 0. \quad (3.1)$$

Rearranging terms,

$$(I + \Delta ti\tilde{A})\hat{\mathbf{v}}^{n+1} + 2\Delta ti\tilde{d}I\hat{\mathbf{v}}^n - (I - \Delta ti\tilde{A})\hat{\mathbf{v}}^{n-1} = 0,$$

where $\tilde{\mathbf{A}} = \mathbf{A}(\tilde{\mathbf{k}})$, $\tilde{d} = d(\tilde{\mathbf{k}})$, and the matrix $\tilde{\mathbf{A}}$ has the same eigenvalues as $\mathbf{A}$ with $\mathbf{k} = (k, l, m)$ replaced by $\tilde{\mathbf{k}} = (\tilde{k}, \tilde{l}, \tilde{m})$. Thus, there exists a unitary matrix $\tilde{\mathbf{P}}$ that diagonalizes the Hermitian matrix $\tilde{\mathbf{A}}$, such that $\tilde{\mathbf{P}}\tilde{\mathbf{A}}\tilde{\mathbf{P}}^{-1} = \tilde{\mathbf{\Lambda}}$ and $\tilde{\mathbf{P}}^{-1} = \tilde{\mathbf{P}}^*$. The transformed system of equations becomes

$$(I + \Delta ti\tilde{\mathbf{\Lambda}})\tilde{\mathbf{P}}\hat{\mathbf{v}}^{n+1} + 2\Delta ti\tilde{d}\tilde{\mathbf{P}}\hat{\mathbf{v}}^n - (I - \Delta ti\tilde{\mathbf{\Lambda}})\tilde{\mathbf{P}}\hat{\mathbf{v}}^{n-1} = 0, \quad (3.2)$$

and to establish the boundedness of the discrete solutions it suffices to show that each component of the transformed vector $\hat{\mathbf{w}} = \tilde{\mathbf{P}}\hat{\mathbf{v}}$ remains bounded, because the transformation itself is norm preserving $\|\tilde{\mathbf{P}}\hat{\mathbf{v}}\| = \|\hat{\mathbf{v}}\|$.

For the advective mode, stability is determined by the leapfrog scheme

$$\hat{w}_j^{n+1} + 2\Delta ti\tilde{d}\hat{w}_j^n - \hat{w}_j^{n-1} = 0 \quad (3.3)$$

with characteristic polynomial

$$z^2 + 2\Delta ti\tilde{d}z - 1 = 0.$$

Solutions are determined by the two roots

$$z_{1,2} = -i\Delta t\tilde{d} \pm (1 - \Delta t^2\tilde{d}^2)^{1/2}.$$

From the constant term of the characteristic polynomial it can be seen that the product of the magnitude of the roots must be 1. Thus for stability both roots must have magnitude 1, which is the case if and only if $1 - \Delta t^2\tilde{d}^2 > 0$, that is,

$$|\Delta t\tilde{d}| \le 1,$$

which ensures that the radicand is positive so the second term will be real. The stability criteria for fast modes can be obtained by examining each eigenvalue of the Fourier transformed version of the discretized system in turn according to the scalar equation

$$(1 + \Delta ti\tilde{\lambda})\hat{w}_j^{n+1} + 2\Delta ti\tilde{d}\hat{w}_j^n - (1 - \Delta ti\tilde{\lambda})\hat{w}_j^{n-1} = 0, \quad (3.4)$$

where $\tilde{\lambda} = \lambda(\tilde{\mathbf{k}})$, with characteristic polynomial

$$(1 + \Delta ti\tilde{\lambda})z^2 + 2\Delta ti\tilde{d}z - (1 - \Delta ti\tilde{\lambda}) = 0.$$

The roots of this quadratic are given by

$$z_{1,2} = \frac{-i\Delta t\tilde{d} \pm (1 + \Delta t^2\lambda^2 - \Delta t^2\tilde{d}^2)^{1/2}}{1 + i\Delta t\tilde{\lambda}}. \quad (3.5)$$

Using a similar argument, Kwizak and Robert (1971) have shown that for stability the product of the magnitudes of the roots again must be 1, which is the case if and only if the radicand is positive:

$$\Delta t^2\tilde{d}^2 \le 1 + \Delta t^2\tilde{\lambda}^2.$$

In order to determine the accuracy of the semi-implicit scheme for both advection and gravity wave modes, the Taylor series expansions of the continuous and discrete amplification factors are compared (see Gustafsson et al. 1995). The continuous (scalar) wave equation in Fourier space and its solution are given by

$$\frac{\partial \hat{w}}{\partial t} + i\lambda\hat{w} = 0, \qquad \hat{w} = e^{-i\lambda t}\hat{w}_0.$$

Solutions of the difference equations (3.3) and (3.4) take the general form

$$\hat{w} = \sigma_1 z_1^n + \sigma_2 z_2^n,$$

where σ_1 and σ_2 are parameters determined by the initial data. One of the two roots represents the computational mode and we assume that the initial data is chosen so that this mode is not excited. Consider the advective eigenvalue $\lambda_R = u_0 k$. The Taylor series expansion of the continuous amplification factor is given by

$$\exp(-i\lambda_R\Delta t) = 1 - iu_0 k\Delta t - \frac{1}{2}u_0^2 k^2\Delta t^2 + O(\Delta t^3)$$

and in the discrete case for roots of the advection equation (3.3) with $\tilde{\lambda}_R = u_0\tilde{k}$

$$z_1 = 1 - iu_0\tilde{k}\Delta t - \frac{1}{2}u_0^2\tilde{k}^2\Delta t^2 + O(\Delta t^3).$$

From the expansion of the approximate wavenumber $\tilde{k}$,

$$k - \tilde{k} = k - k\,\frac{\sin(k\Delta x)}{k\Delta x} = -\frac{k^3\Delta x^2}{6} + O(\Delta x^4)$$

and it follows that

$$\exp(-i\lambda_R\Delta t) = z_1 + O(k^3\Delta x^2\Delta t).$$

It is well known that the use of approximately ten spatial mesh points per wave provides reasonable numerical accuracy of a second-order finite-difference approximation of a spatial derivative (Gustafsson et al. 1995). In the numerical approximation of the scaled system this is equivalent to choosing $\Delta x = O(\varepsilon)$. The Courant condition for the advective mode is $\Delta t < \Delta x/\max\tilde{d}$, and because $\max\tilde{d} = O(1)$, this means that Δt must be $O(\varepsilon)$ in order to satisfy the Courant condition. In that case there are also approximately 10 points per temporal wavenumber for the advective mode; that is, the numerical approximations of the time derivative of the advective mode should also be accurate. Based on this logic, it seems reasonable to expect that this same time step might also produce accurate approximations of the temporal derivatives of the long gravity waves that are produced by slowly evolving in time mesoscale heating because those waves have the same timescale as the advective mode (Browning and Kreiss 1997). The main result of our paper is that the long gravity waves, with $k = \varepsilon k'$ where k' is $O(1)$, are accurately reproduced with a time step that provides reasonable accuracy for the advective mode. The Taylor series expansion of the discrete amplification factor for the semi-implicit scalar equation (3.4) is given by

$$z_1 = 1 - i\varepsilon^{-1}\tilde{\lambda}_g\Delta t - \frac{1}{2}\varepsilon^{-2}\tilde{\lambda}_g^2\Delta t^2 + O(\Delta t^3).$$

The above expansion is only valid when the following series converge inside the unit disc in the complex plane. In the denominator of (3.5), let $z = i\varepsilon^{-1}\tilde{\lambda}_g\Delta t$

$$\frac{1}{1+z} = 1 - z + O(z^2), \qquad |z| < 1$$

and in the numerator $z = \varepsilon^{-2}\tilde{\lambda}_g^2\Delta t^2$,

$$(1+z)^{1/2} = 1 + \frac{1}{2}z + O(z^2), \qquad |z| < 1.$$

Thus for large-scale gravity waves, $\lambda_g(\tilde{k} = \varepsilon)$ have an $O(\varepsilon)$ error and $\lambda_g(\tilde{k} = 1)$ have an $O(1)$ error. If Δt is chosen to be $O(\varepsilon)$, then convergence is assured for $\tilde{k} = \varepsilon\tilde{k}'$. For these gravity waves

$$\lambda_g - \tilde{\lambda}_g = O(k^3\Delta x^2)$$

and therefore

$$\exp(-i\lambda_g\Delta t) = z_1 + O(k^3\Delta x^2\Delta t).$$

To obtain the truncation error from the continuous $\mathbf{P}\hat{\mathbf{u}}$ and discrete $\tilde{\mathbf{P}}\hat{\mathbf{v}}$ vectors in Fourier space, first introduce the discretization operators

$$D_t(\psi) = \frac{\psi^{n+1} - \psi^{n-1}}{2\Delta t}, \qquad \mu_t(\psi) = \frac{\psi^{n+1} - \psi^{n-1}}{2}.$$

The continuous wave equation with forcing is given by

$$\frac{\partial \hat{\mathbf{u}}}{\partial t} + i\mathbf{A}(\mathbf{k})\hat{\mathbf{u}} + idI\hat{\mathbf{u}} - \hat{\mathbf{f}} = 0 \tag{3.6}$$

and the corresponding time and space discretized system is

$$D_t\hat{\mathbf{v}} + i\mathbf{A}(\tilde{\mathbf{k}})\,\mu_t\hat{\mathbf{v}} + i\tilde{d}I\hat{\mathbf{v}}^n - \hat{\mathbf{f}} = 0. \tag{3.7}$$

The truncation error τ is obtained by substituting $\hat{\mathbf{u}}$ into this equation

$$D_t\hat{\mathbf{u}} + i\mathbf{A}(\tilde{\mathbf{k}})\,\mu_t\hat{\mathbf{u}} + i\tilde{d}I\hat{\mathbf{u}} - \hat{\mathbf{f}} = \tau. \tag{3.8}$$

In transformed variables, expand each term above as follows:

$$\tilde{\mathbf{P}}^{-1}(D_t\tilde{\mathbf{P}}\hat{\mathbf{u}}) = \tilde{\mathbf{P}}^{-1}[D_t\mathbf{P}\hat{\mathbf{u}} + (\tilde{\mathbf{P}} - \mathbf{P})\mathbf{P}^{-1}D_t\mathbf{P}\hat{\mathbf{u}}]$$

$$\tilde{\mathbf{P}}^{-1}(\tilde{\mathbf{P}}\tilde{\mathbf{A}}\tilde{\mathbf{P}}^{-1}\mu_t\tilde{\mathbf{P}}\hat{\mathbf{u}}) = \tilde{\mathbf{P}}^{-1}[\mathbf{\Lambda}\mu_t\mathbf{P}\hat{\mathbf{u}} + (\tilde{\mathbf{\Lambda}} - \mathbf{\Lambda})\mu_t\mathbf{P}\hat{\mathbf{u}} + \tilde{\mathbf{\Lambda}}(\tilde{\mathbf{P}} - \mathbf{P})\mu_t\hat{\mathbf{u}}]$$

$$\tilde{\mathbf{P}}^{-1}(\tilde{d}\tilde{\mathbf{P}}\hat{\mathbf{u}}) = \tilde{\mathbf{P}}^{-1}[d\mathbf{P}\hat{\mathbf{u}} + (\tilde{d} - d)\mathbf{P}\hat{\mathbf{u}} + \tilde{d}(\tilde{\mathbf{P}} - \mathbf{P})\hat{\mathbf{u}}]$$

$$\tilde{\mathbf{P}}^{-1}(\tilde{\mathbf{P}}\hat{\mathbf{f}}) = \tilde{\mathbf{P}}^{-1}[\mathbf{P}\hat{\mathbf{f}} + (\tilde{\mathbf{P}} - \mathbf{P})\hat{\mathbf{f}}],$$

where the large terms satisfying (3.6) drop out and it has been shown that

$$\mathbf{\Lambda}(\tilde{\mathbf{k}}) - \mathbf{\Lambda}(\mathbf{k}) = O(\Delta x^2), \qquad \tilde{d} - d = O(\Delta x^2).$$

The Taylor series expansion of $\tilde{P}$ is

$$\mathbf{P}(\tilde{\mathbf{k}}) = \mathbf{P}(\mathbf{k}) + \mathbf{P}_{\mathbf{k}}(\mathbf{k})(\tilde{\mathbf{k}} - \mathbf{k}) + O(\tilde{\mathbf{k}} - \mathbf{k})^2,$$

where

$$\mathbf{P}(\tilde{\mathbf{k}}) - \mathbf{P}(\mathbf{k}) = O(\tilde{\mathbf{k}} - \mathbf{k}) = O(\Delta x^2)$$

assuming $\mathbf{P}_{\mathbf{k}}$ is bounded for fixed $\mathbf{k}$. Here assume that there is no energy in the variables and waves where we cannot prove that the truncation error is small. This implies the application of proper initialization procedures even for the semi-implicit method. Therefore, in transformed variables (3.8) becomes

$$\tilde{\mathbf{P}}^{-1}[O(\Delta x^2) + O(\Delta t^2)] = O(\Delta x^2) + O(\Delta t^2).$$

Now define $\hat{\mathbf{e}} = \hat{\mathbf{u}} - \hat{\mathbf{v}}$, the resulting error equation is given by

$$\tilde{\mathbf{P}}^{-1}[D_t\mathbf{P}\hat{\mathbf{e}} + i\mathbf{A}(\tilde{\mathbf{k}})\mu_t\mathbf{P}\hat{\mathbf{e}} + i\tilde{d}\mathbf{P}\hat{\mathbf{e}}] = O(\Delta x^2) + O(\Delta t^2), \tag{3.9}$$

where the forcing is replaced by the truncation error. Assuming the error at the initial time is zero and stability of the finite-difference method, by Duhamel's principle the error will be of the size of the forcing.

4. Numerical algorithms

Space discretization operators are the forward D_+ and backward D_- differences and average μ_ψ on a staggered Arakawa C grid in the horizontal direction and Lorenz grid in the vertical direction. Thus, scalar quantities are located at grid cell centers, whereas vector components are on cell faces. Time discretization operators appearing in the leapfrog or three-time-level semi-implicit scheme are given by

$$D_t(\psi) = \frac{\psi^{n+1} - \psi^{n-1}}{2\Delta t},$$

$$\mu_t(\psi) = \frac{\psi^{n+1} + \psi^{n-1}}{2} = \Delta t D_t(\psi) + \psi^{n-1}.$$

Therefore, a fully 3D semi-implicit scheme applied to the compressible governing equations in dimensional form results in

$$\begin{aligned}
D_t(u) + \mu_t\rho_0^{-1}D_{x-}(p') &= f_u^n \\
D_t(v) + \mu_t\rho_0^{-1}D_{y-}(p') &= f_v^n \\
D_t(w) + \mu_t(\overline{\rho_0}^z)^{-1}D_{z-}(p') - \mu_t B(s', p') &= f_w^n \\
D_t(p') + \gamma p_0\mu_t D - \mu_t g\rho_0\mu_z(w) &= f_{p'}^n \\
D_t(s') - \frac{N_0^2}{g}\mu_t\mu_z(w) &= f_{s'}^n,
\end{aligned}$$

where the f_ψ^n contain nonlinear advection, Coriolis, and mixing terms. Time averages are replaced by differences to avoid numerical cancellation (Laprise and Girard 1990) and thus only time tendencies appear on the left-hand side. The remaining terms at time level $n-1$ are placed on the right-hand side of the equations:

$$D_t(u) + \Delta t\rho_0^{-1}D_{x-}D_t(p') = q_u \tag{4.1}$$

$$D_t(v) + \Delta t\rho_0^{-1}D_{y-}D_t(p') = q_v \tag{4.2}$$

$$D_t(w) + \Delta t(\overline{\rho_0}^z)^{-1}D_{z-}D_t(p') - \Delta t D_t B(s', p') = q_w \tag{4.3}$$

$$D_t(p') + \Delta t\gamma p_0 D_t D - \Delta t g\rho_0\mu_z D_t(w) = q_{p'} \tag{4.4}$$

$$D_t(s') - \Delta t\frac{N_0^2}{g}\mu_z D_t(w) = q_{s'}, \tag{4.5}$$

where the right-hand sides now become

$$\begin{aligned}
q_u &= f_u^n - \rho_0^{-1}D_{x-}(p')^{n-1} \\
q_v &= f_v^n - \rho_0^{-1}D_{y-}(p')^{n-1} \\
q_w &= f_w^n - (\overline{\rho_0}^z)^{-1}D_{z-}(p')^{n-1} + B(s', p')^{n-1} \\
q_{p'} &= f_{p'}^n - \gamma p_0 D^{n-1} + g\rho_0\mu_z(w)^{n-1} \\
q_{s'} &= f_{s'}^n + \frac{N_0^2}{g}\mu_z(w)^{n-1}.
\end{aligned}$$

To obtain an implicit system of equations for the pressure perturbation p', we proceed to eliminate all other prognostic variables from Eqs. (4.1)–(4.5). Eliminating the buoyancy B and horizontal divergence D_h from the system of equations results in

$$(1 + \Delta t^2\mu_z N_0^2\mu_z)D_t(w) + \Delta t\left(\frac{1}{\overline{\rho_0}^z}D_{z-} + \mu_z\frac{g}{\gamma p_0}\right)D_t(p') = q_w^* \tag{4.6}$$

$$\left(\frac{1}{\gamma p_0} - \Delta t^2\frac{1}{\rho_0}\nabla_h^2\right)D_t(p') + \Delta t\left(D_{z+} - \frac{g}{c_0^2}\mu_z\right)D_t(w) = q'_{p'}, \tag{4.7}$$

where

$$q_w^* = q_w - \Delta t g\mu_z q_{s'}, \qquad q'_{p'} = \frac{1}{\gamma p_0}q_{p'} - \Delta t D_h(q_u, q_v).$$

Define the operators

$$\mathcal{N} = (1 + \Delta t^2 \mu_z N_0^2 \mu_z), \qquad D_z^{(1)} = \left(\frac{1}{\overline{\rho_0}^z} D_{z-} + \mu_z \frac{g}{\gamma p_0}\right),$$

$$D_z^{(2)} = \left(D_{z+} - \frac{g}{c_0^2}\mu_z\right).$$

Solving directly for $D_t(w)$

$$D_t(w) + \Delta t \mathcal{N}^{-1} D_z^{(1)} D_t(p') = \mathcal{N}^{-1} q_w^* \quad (4.8)$$

$$\frac{1}{\rho_0}\left(\frac{1}{c_0^2} - \Delta t^2 \nabla_h^2\right) D_t(p') + \Delta t D_z^{(2)} D_t(w) = q_{p'}'. \quad (4.9)$$

Substitute (4.8) into (4.9) to obtain the discrete equation, approximating the elliptic structure equation

$$\frac{1}{\rho_0}\left(\frac{1}{c_0^2} - \Delta t^2 \nabla_h^2\right) D_t(p') - \Delta t^2 D_z^{(2)} \mathcal{N}^{-1} D_z^{(1)} D_t(p') = q_p^*, \quad (4.10)$$

where

$$q_{p'}^* = q_{p'}' - \Delta t\, D_z^{(2)} \mathcal{N}^{-1} q_w^*.$$

The remaining tendencies are obtained by back substitution as follows:

$$D_t(u) = q_u - \Delta t \rho_0^{-1} D_{x-} D_t(p') \quad (4.11)$$

$$D_t(v) = q_v - \Delta t \rho_0^{-1} D_{y-} D_t(p') \quad (4.12)$$

$$D_t(w) = \mathcal{N}^{-1}[q_w^* - \Delta t D_z^{(1)} D_t(p')] \quad (4.13)$$

$$D_t(s') = q_{s'} + \Delta t \frac{N_0^2}{g} \mu_z D_t(w). \quad (4.14)$$

The discrete elliptic operator appearing in Eq. (4.10) is separable. The vertical operator is tridiagonal and has constant coefficients for an isothermal atmosphere. A direct linear system solver can be applied, which is based on fast tensor-product techniques (Swarztrauber 1985). In the case of periodic boundary conditions, the eigenvalues of the horizontal Laplacian operator can be easily determined and precomputed. Application of a (real to complex) fast Fourier transform (FFT) to (4.10) in each of the horizontal directions leads to a sequence of tridiagonal systems to solve in the vertical direction. Given an $N_x \times N_y \times N_z$ grid, these tridiagonal systems take the form

$$\frac{1}{\rho_0}\left[\frac{1}{c_0^2} - \Delta t^2(\lambda_l + \lambda_m)\right] D_t(\widehat{p'}) - \Delta t^2 D_z^{(2)} \mathcal{N}^{-1} D_z^{(1)} D_t(\widehat{p'}) = \widehat{q_p^*}, \quad (4.15)$$

where

$$\lambda_l = -\frac{4}{\Delta x^2} \sin^2\left(\frac{\pi l}{N_x}\right), \qquad l = 0, \ldots \lfloor N_x/2 \rfloor,$$

$$\lambda_m = -\frac{4}{\Delta y^2} \sin^2\left(\frac{\pi m}{N_y}\right), \qquad m = 0, \ldots \lfloor N_y/2 \rfloor$$

are the eigenvalues of the discrete horizontal Laplacian operator in the x and y directions. The solution in physical space is obtained by applying the inverse FFT to the solutions. Assuming $N_x = N_y = N_z$, the 2D FFT requires $O(N^3 \log N)$ floating point operations (flops), whereas the vertical solves involve $O(N^3)$ flops. Therefore the dominant cost of the semi-implicit time-stepping scheme is associated with the FFT computation within the elliptic solver. Multigrid solvers are a possible alternative with an optimal complexity of $O(N^3)$ but can have a large constant factor depending on the problem. It should be emphasized at this point that a constant coefficient linear system is obtained by assuming that the pressure and density perturbations remain small compared to the reference state and thus we use ρ_0 in the momentum equations instead of linearizing every time step with ρ^n. Furthermore, topography has not been introduced into the model because we are primarily interested in the accurate simulation of gravity waves generated by mesoscale storms. For gravity waves with wavelengths larger than the characteristic length scale of the heating, the semi-implicit scheme accurately reproduces an explicit simulation at a fraction of the computational cost. If the accurate simulation of long gravity waves is not essential, then the reduced system of Browning and Kreiss (1997) provides an even faster alternative. The reduced scheme has a computational cost of $O(N^2)$ to advance the momentum equations (hyperbolic part) and $O(N^2 \log N)$ per vertical level to solve a Poisson problem or $O(N^3 \log N)$ overall. Although the reduced system model has the same operation count as the semi-implicit model, the constant factor is much smaller because there are fewer equations and there is less averaging.

5. Numerical examples

Following Browning and Kreiss (1997), a number of the theoretical results in the previous sections can be demonstrated by specifying a heating function $H(x, y, z, t)$ that has spatial and temporal distributions similar to those observed in the atmosphere. In particular, they chose $H = H_0 H_1(x, y) H_2(z) H_3(t)$, where

$$H_0 = 0.5 \text{ m s}^{-1}, \quad (5.1)$$

$$H_1(x, y) = \exp\{-[(x - L/2)^2 + (y - L/2)^2]/r_e^2\}, \qquad r_e = 50 \times 10^3 \text{ m}, \quad (5.2)$$

$$H_2(z) = \sin(2\pi z/D), \quad (5.3)$$

$$H_3(t) = e^{-(t - 6 \cdot 3600)^2/(2 \cdot 3600)^2}, \quad (5.4)$$

$L = 900 \times 10^3$ m is the length and width of the domain, and $D = 12 \times 10^3$ m is the depth. The lateral dimensions of the domain were intentionally chosen to be considerably larger than that of the heating to allow the gravity waves to behave more as they would in the real atmosphere. The spatial component of the heating $H_0 H_1 H_2$

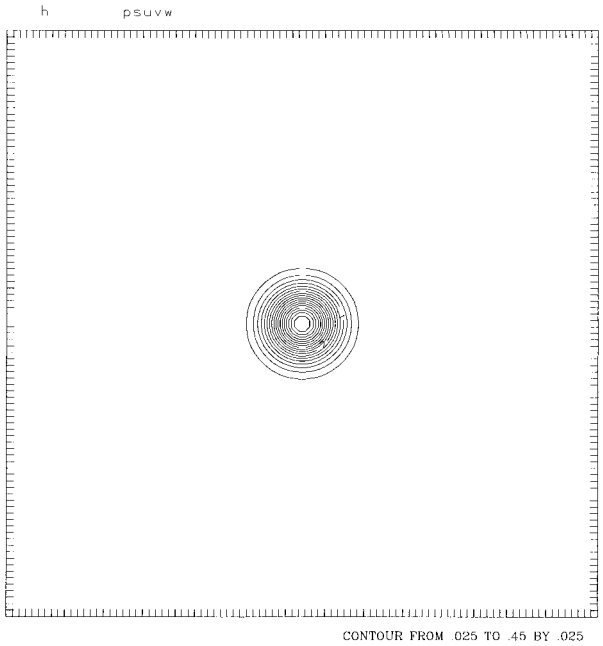

FIG. 1. The spatial component of the heating $H_0H_1H_2$ at $z = 9$ km. The contour interval is 0.025 m s^{-1}.

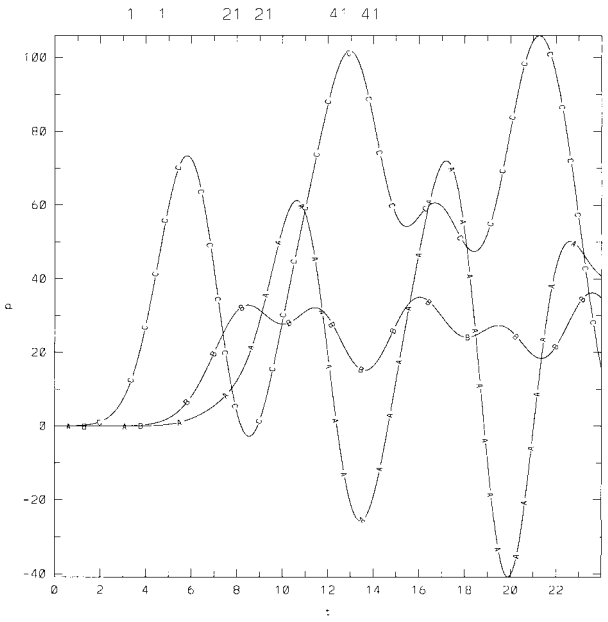

FIG. 2. The pressure perturbation p' (Pa) from the explicit model ($\Delta t = 1$ s) plotted at the grid points A = (1, 1, 1), B = (21, 21, 1), and C = (41, 41, 1) as a function of time (h).

(m s^{-1}) at $z = 9$ km is shown in Fig. 1 and should be compared with the stratiform rain region of Houze's schematic of a typical mesoscale convective system (Houze 1989, his Fig. 1). Houze states that the magnitude of the vertical velocity in a wide range of MCS is on the order of 0.1–0.5 ms^{-1}. For slowly varying solutions of (2.1)–(2.5), the maximum vertical velocity is determined by the maximum value of H and from (5.1) that will be 0.5 m s^{-1}. The time dependence of the heating (5.4) is a Gaussian distribution centered at 6 h with an e-folding parameter of 2 h.

In earlier work (Browning and Kreiss 1997) the accuracy of the reduced system model was demonstrated by computing the solutions of the full model using an explicit time-stepping scheme and showing the differences between the two remained small as predicted by the mathematical theory. It was also found that the explicit model solutions compared favorably with those produced by the multiscale model. Here we show that the semi-implicit time-stepping scheme described in section 4 can also accurately simulate gravity waves with wavelengths larger than the characteristic length scale of the heat source. Explicit simulations of a model based on the full system will be compared against the semi-implicit scheme for the forcing specified above. As in the earlier study, it is assumed that the Coriolis parameter is $f = 10^{-4}$ s^{-1} and that the lateral boundary conditions are periodic. The reference state is computed from an isothermal atmosphere whose reference temperature is 340 K. The top of the model domain is a rigid lid and there is no topography. The computational grid consists of $90 \times 90 \times 12$ points corresponding to a horizontal resolution of $\Delta x = \Delta y = 10$ km. A Robert filter (Asselin 1972) was not needed to produce these results. For stability, the time step was set to $\Delta t = 1$ s in the explicit model runs, whereas $\Delta t = 300$ s was possible in the semi-implicit simulations because of the small advection speeds in this example.

Figures 2 and 3 are plots from the explicit model of

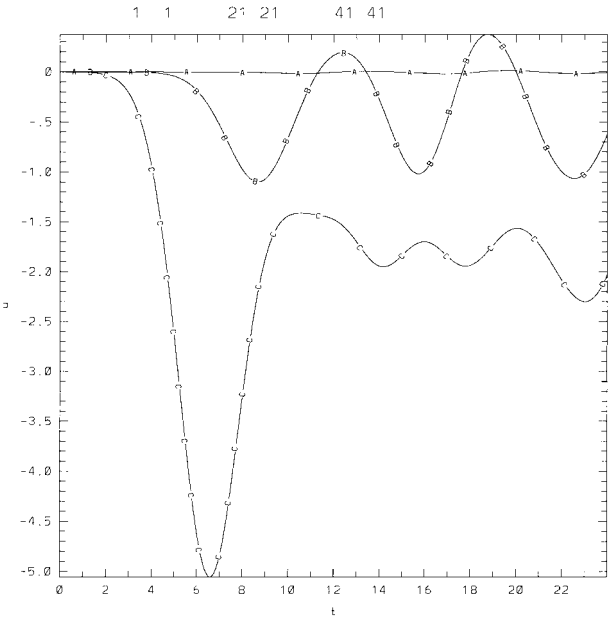

FIG. 3. The eastward component of the velocity u (m s^{-1}) from the explicit model ($\Delta t = 1$ s) plotted at the grid points A = (1, 1, 1), B = (21, 21, 1), and C = (41, 41, 1) as a function of time (h).

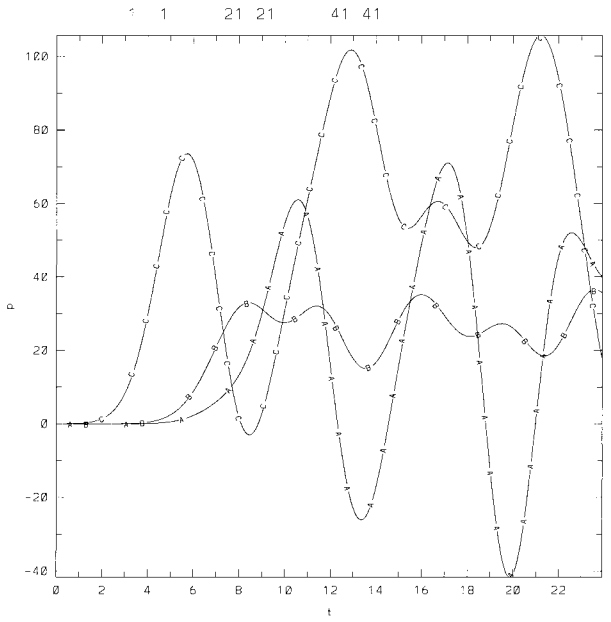

FIG. 4. The pressure perturbation p' (Pa) from the semi-implicit model (Δt = 300 s) plotted at the grid points A = (1, 1, 1), B = (21, 21, 1), and C = (41, 41, 1) as a function of time (h).

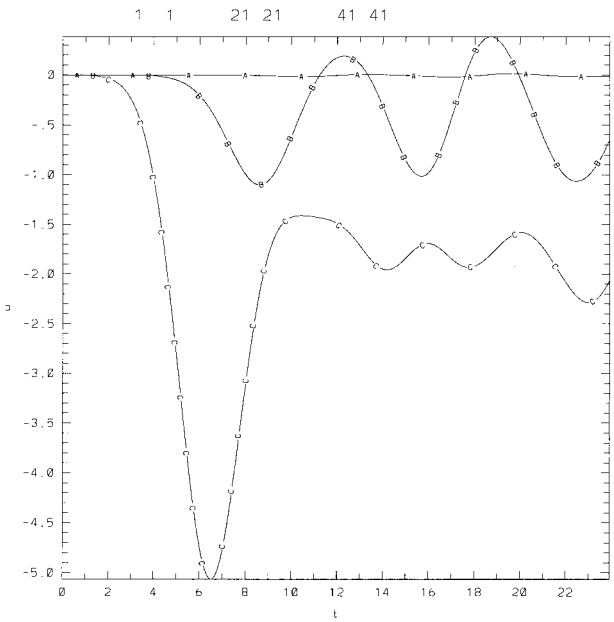

FIG. 5. The eastward component of the velocity u (m s^{-1}) from the semi-implicit model (Δt = 300 s) plotted at the grid points A = (1, 1, 1), B = (21, 21, 1), and C = (41, 41, 1) as a function of time (h).

the pressure perturbation p (Pa) and eastward component of the wind u (m s^{-1}) at the three grid points with indices A = (1, 1, 1), B = (21, 21, 1), and C = (41, 41, 1) as a function of time. Point *A* is at the lower-left corner of the domain (as far away from the storm as possible), point B is approximately halfway along the line from point A to the center point at this level, and point C is on the same line close to the center of the storm. Note that the pressure at point C increases as the storm intensifies and then decreases as the storm subsides after 6 h. Also the pressure has a period roughly the same as the period of the heating (≈6–7 h) and the dominant component of the solution reaches a steady state after about 12 h, so all the oscillations in the pressure and velocity after that time are mainly due to gravity waves. The vertical velocity (Browning and Kreiss 1997, their Fig. 7) in the storm decreases in magnitude as the storm diminishes as expected. The magnitude of the deviations of the vertical velocity from the gravity wave component of the solution (0.03 m s^{-1}) is an order of magnitude smaller than the maximum magnitude of the dominant component of the solution (0.5 m s^{-1}).

The semi-implicit simulation results for the pressure perturbation p (Pa) and eastward component of the wind u (m s^{-1}) are plotted in Figs. 4 and 5 at the three grid points, A, B, and C. The results are essentially identical when compared with the explicit runs. To emphasize that only large-scale gravity waves were generated in both model runs, Fig. 6 is a contour plot of the pressure perturbation at the surface at 24 h. The scale of the gravity waves is clearly much larger than the heating term shown in Fig. 1. In order to verify that the scaling arguments in section 2 are valid for the specified forcing function, small terms in the linear system (4.10) corresponding to small terms in the gravity wave equation (2.10) were dropped for a third model run. As expected, the computed solution closely follows the explicit and semi-implicit solutions. In order to compare the computational requirements of the semi-implicit and reduced

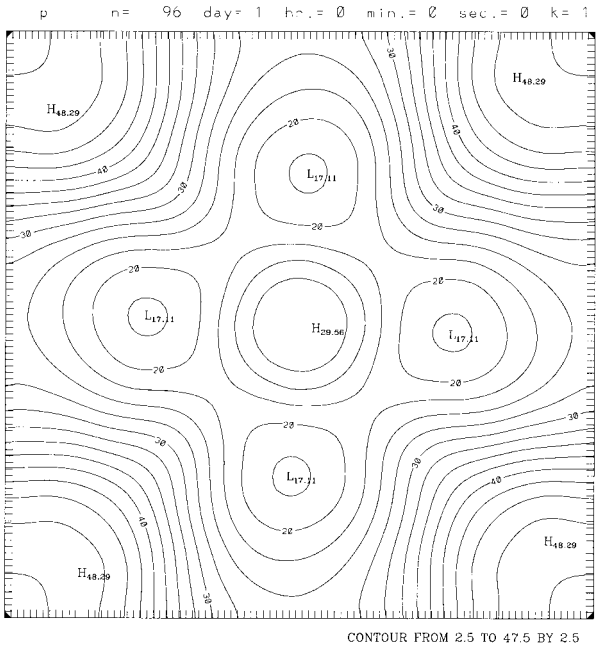

FIG. 6. The pressure perturbation at the surface from the semi-implicit model at 24 h. Contour interval is 2.5 Pa.

models, both codes were run on an SGI Origin 2000 computer at the National Center for Atmospheric Research. The reduced model was run with $\Delta t = 300$ s and required 0.6 s for a single level run of 24 h. An estimate of the time for a 12-level run is $12 \times 0.6 = 7.2$ s. The semi-implicit scheme was also run with $\Delta t = 300$ s for 24 h and required 70 s. Therefore, the reduced system model is ten times faster than the semi-implicit model. It should be noted, however, that the reduced model employs a nonstaggered Arakawa A grid whereas the semi-implicit model is discretized on a C grid.

6. Conclusions

In this paper we have shown that a fully 3D semi-implicit time-stepping scheme can accurately reproduce gravity waves with wavelengths larger than the characteristic length scale of the heat source in a mesoscale storm at midlatitudes. The reduced system model of Browning and Kreiss (1997) can reproduce the dominant component of the solution, which contains most of the energy in the vicinity of the storm that is meteorologically significant. The computing time for the reduced model is ten times faster than the 3D semi-implicit model for a mesoscale convective system. However, the reduced system is only useful if studying a mesoscale storm in isolation when no large-scale features are present in the same domain. It should also be noted that the presence of strong jets in the model domain could reduce the advantage of both the semi-implicit and reduced models. If we consider the case of the multiscale model (Browning and Kreiss 1986), with $\alpha = (\Delta z/\Delta x)^2$, then for the mesoscale case this factor is $(10^4 \text{ m}/10^5 \text{ m})^2 = 10^{-1}$ so the time step is a factor of 10 larger than the explicit case ($\alpha = 1$). This makes the multiscale model more competitive with the semi-implicit model in the realistic case when jets are present, that is, then the ratio of the time steps should just be that of the horizontal sound speed divided by the jet speed ($300 \text{ m s}^{-1}/100 \text{ m s}^{-1} = 3$). As long as the elliptic solver is sufficiently fast, the semi-implicit method will be faster than the multiscale model. But if the introduction of topography necessitates the use of an iterative elliptic solver such as GMRES (Saad and Schultz 1986; Skamarock et al. 1997; Thomas et al. 1998), then this may not be the case. We plan to address this issue and the question of open boundary conditions for a 3D semi-implicit discretization in future papers.

Acknowledgments. The authors would like to thank Paul Swarztrauber and Richard Valent of NCAR/SCD for their advice on the use of FFTPACK 5 in the construction of fast elliptic solvers. We would also like to thank Prof. Geoffrey Vallis and two anonymous reviewers for their comments and suggestions. They have improved the presentation and interpretation of our results.

REFERENCES

Asselin, R. A., 1972: Frequency filter for time integrations. *Mon. Wea. Rev.,* **100,** 487–490.

Browning, G. L., and H.-O. Kreiss, 1986: Scaling and computation of smooth atmospheric motions. *Tellus,* **38A,** 295–313.

——, and ——, 1994: The impact of rough forcing on systems with multiple time scales. *J. Atmos. Sci.,* **51,** 369–383.

——, and ——, 1997: The role of gravity waves in slowly varying in time mesoscale motions. *J. Atmos. Sci.,* **54,** 1166–1184.

——, ——, and W. H. Schubert, 2000: The role of gravity waves in slowly varying in time tropospheric motions near the equator. *J. Atmos. Sci.,* **57,** 4008–4019.

Cullen, M. J. P., 1990: A test of a semi-implicit integration technique for a fully compressible nonhydrostatic model. *Quart. J. Roy. Meteor. Soc.,* **116,** 1253–1258.

Elvius, T., and A. Sundström, 1973: Computationally efficient schemes and boundary conditions for a fine-mesh barotropic model based on the shallow-water equations. *Tellus,* **25,** 132–156.

Golding, B. W., 1992: An efficient nonhydrostatic forecast model. *Meteor. Atmos. Phys.,* **50,** 89–103.

Gustafsson, B., H.-O. Kreiss, and J. Oliger, 1995: *Time Dependent Problems and Difference Methods*. Wiley, 572 pp.

Houze, R. A., 1989: Observed structure of mesoscale convective systems and implications for large-scale heating. *Quart. J. Roy. Meteor. Soc.,* **115,** 425–461.

Johansson, O., and H.-O. Kreiss, 1963: Über das Verfahren der zentralen Differenzen zur Lösung des Cauchyproblems für partielle Differentialgleichungen (in German). *BIT,* **3,** 97–107.

Kreiss, H.-O., 1979: Problems with different time scales for ordinary differential equations. *SIAM J. Numer. Anal.,* **16,** 980–998.

——, 1980: Problems with different time scales for partial differential equations. *Commun. Pure Appl. Math.,* **33,** 399–440.

Kwizak, M., and A. J. Robert, 1971: A semi-implicit scheme for grid point atmospheric models of the primitive equations. *Mon. Wea. Rev.,* **99,** 32–36.

Laprise, R., and C. Girard, 1990: A spectral general circulation model using a piecewise-constant finite-element representation on a hybrid vertical coordinate system. *J. Climate,* **3,** 32–52.

Robert, A. J., 1969: The integration of a spectral model of the atmosphere by the implicit method. *Proc. WMO-IUGG Symp. on Numerical Weather Prediction*, Vol. VII, Tokyo, Japan, Japan Meteorological Agency, 19–24.

——, 1993: Bubble convection experiments with a semi-implicit formulation of the Euler equations. *J. Atmos. Sci.,* **50,** 1865–1873.

Saad, Y., and M. Schultz, 1986: GMRES: A generalized minimal residual algorithm for solving nonsymmetric linear systems. *SIAM J. Sci. Stat. Comput.,* **7,** 856–869.

Skamarock, W. C., P. K. Smolarkiewicz, and J. B. Klemp, 1997: Preconditioned conjugate residual solvers for Helmholtz equations in nonhydrostatic models. *Mon. Wea. Rev.,* **125,** 587–599.

Swarztrauber, P., 1985: Fast poisson solvers. *Studies in Numerical Analysis*, G. H. Golub, Ed., MAA Studies in Mathematics, Vol. 24, Math Association of America, 319–369.

Tanguay, M., A. Robert, and R. Laprise, 1990: A semi-implicit semi-Lagrangian fully compressible regional forecast model. *Mon. Wea. Rev.,* **118,** 1970–1980.

Tapp, M. C., and P. W. White, 1976: A nonhydrostatic mesoscale model. *Quart. J. Roy. Meteor. Soc.,* **102,** 277–296.

Thomas, S. J., C. Girard, R. Benoit, M. Desgagné, and P. Pellerin, 1998: A new adiabatic kernel for the MC2 model. *Atmos.–Ocean,* **36,** 241–270.

Williamson, D. L., and R. Laprise, 1999: Numerical approximations for global atmospheric general circulation models. *Numerical Modelling of the Global Atmosphere in the Climate System*, P. W. Mote and A. O'Neill, Eds., NATO Advanced Study Institute Proceedings, Kluwer Academic.